# A Fluid-Structure Interaction Simulation by Smoothed Particle Hydrodynamics

Mehrdad H. Farahani, Nima Amanifard, S. Majid Hosseini

*Abstract—* **It is still difficult for traditional methods to simulate fluid-structure interaction (FSI) problems which are increasingly used to model cardiovascular system, and human organism. This contribution develops a new numerical method to analyze FSI, based on smoothed particle hydrodynamics (SPH). The Lagrangian and meshless characteristics of SPH presents distinct features to devise the method by which both fluid and elastic structure continua are coupled using a monolithic but explicit numerical algorithm. The method consists of a predictor-corrector scheme in which the first step plays the role of prediction, whereas in the second step velocity field is corrected according to the incompressibility constraint. The no-slip boundary condition is imposed on deformable walls by projecting the fluid velocities on ghost particles which carry with solid particles at the interface boundary. The method is employed to simulate pulsatory flow of an isothermal and incompressible fluid moving through flexible walls.**

*Index Terms—* **Smoothed particle hydrodynamics (SPH), Fluid-structure interaction (FSI), Lagrangian method, no-slip boundary condition**

## I. INTRODUCTION

Fluid-structure interaction (FSI) problems are of multiphysics phenomena in which two or more different, yet interrelated fluid and solid domain interact with each other as a unit. Considering the advancement of powerful computers thereby large amount of computation can be performed, numerical modelling of such challenging problems in which the interface boundaries are deformable, have became increasingly important in recent years. For instance, such numerical methods provide a valuable tool in biomechanical applications so that computational modelling has facilitated the progress of hemodynamics and cardiovascular researches.

Although there are several successful methods to solve FSI problems, there is no general strategy by which all FSI problems can be addressed. A basic problem associated with these numerical methods is selection of the reference frame in which each of solid and fluid domains are solved. Conventionally, fluid domain is solved based on Eulerian

Manuscript received March 3, 2008.

M. H. Farahani is with Department of Mechanical Engineering, Faculty of Engineering, University of Guilan, Rasht, 3756 IRAN (e-mail: mh.farahani@gmail.com).

N. Amanifard is with Department of Mechanical Engineering, Faculty of Engineering, University of Guilan, Rasht, 3756 IRAN. (Corresponding author; phone: 98-131-6690274-8; fax: 98-131-6690271; e-mail: namanif@guian.ac.ir).

S. M. Hosseini is with Department of Chemical and Biological Engineering, University of British Colombia, Vancouver V6T 1Z3 CANADA, (shosseini@chml.ubc.ca).

description, whereas Lagrangian approach is the preferred method for simulation of the solid domain. The foregoing descriptions are mathematically dissimilar considering the nonlinear convective term which appears in the momentum equation in Eulerian framework.

From the other view point, numerical methods, which are conventionally utilized to model FSI, are generally based on tessellation of the solution domain by grids, or mesh. Grids quality plays a crucial role in simulations of grid-based methods so that the accuracy of simulations is highly affected by grid configuration. Furthermore, regarding FSI problems where interaction of fluid and elastic structure is desirable, the evaluation of field variables on deformable boundaries considerably affects the accuracy of the result. Generally, there are two classes of grid-based methods namely fixed-grid methods and deforming-grid methods [1]. Deforming-grid methods usually need remeshing, particularly when large deformation is of great interest; however, remeshing strategy can be a difficult and time consuming task [1,2]. On the other hand, fixed-grid methods often require an interpolation to the immersed boundary, which results in inaccurate computations in vicinity of these boundaries [2].

Smoothed particle hydrodynamics (SPH) is a Lagrangian particle method in which a set of bulk (moving or stationary) fluids and/or solids are employed as an alternative for grids. During two past decades, SPH has employed to simulate incompressible fluids as well as elastic-plastic deformations. Recently, some researches have been devoted to utilize SPH to simulate FSI problems [3,4,5]. Antoci *et al*. [3] used standard SPH along with an incremental hypoelastic relation to simulate FSI problems. On the other hand, Hosseini *et al*. [4] developed a three-step SPH algorithm, which had already been proposed by Hosseini *et al*. [6], to simulate FSI problems. In addition, viscosity was taken into account in their simulations; whereas, neither artificial viscosity nor artificial stress was used. Comparing these two methods illustrates that the results reported by Hosseini *et al*. [4], in deformation of an elastic gate subjected to water pressure, were more accurate than the results which were reported by Antoci *et al*. [3]. Farahani *et al*. [5] also employed the three-step method aforementioned to simulate FSI with complex free surface flows.

Indeed, neither Hosseini et al. [4] nor Antoci et al. [3] considered the no-slip boundary conditions in their simulations. In the current work, the problem of imposing the no-slip boundary condition on moving walls is studied. In this way, the three-step algorithm of Hosseini et al. [4,6] is modified according to the viscosity term proposed by Morris

et al. [7]. In order to investigate the accuracy of the modified algorithm, a poiseuille flow is simulated and velocity profile is compared with analytical solution. Moreover, the method is used to simulate an internal pulsatory flow moving through flexible walls.

## II. GOVERNING EQUATIONS

### A. Fluid domain

The fluid is assumed to be isothermal and incompressible, and the governing equations within the fluid domain in absence of body forces, are given by

$$\frac{D\rho}{Dt} = -\rho \frac{\partial u^j}{\partial x^j} \tag{1}$$

$$\frac{Du^i}{Dt} = \frac{1}{\rho} \frac{\partial \tau^{ij}}{\partial x^j} - \frac{1}{\rho} \frac{\partial P}{\partial x^j} \tag{2}$$

where $\rho$, $t$, $p$, $u^j$, and $\tau^{ij}$ denotes the density, time, pressure, velocity vector, and shear stress tensor respectively. Moreover, $x^j$ is the $j$ th component of position vector.

### B. Solid domain

The momentum equation for an elastic body in absence of body forces is

$$\frac{Du^i}{Dt} = \frac{1}{\rho} \frac{\partial \sigma^{ij}}{\partial x^j}, \tag{3}$$

where $\sigma^{ij}$ is the stress tensor,

$$\sigma^{ij} = -P\delta^{ij} + S^{ij}, \tag{4}$$

where $S^{ij}$ is the deviatoric stress tensor. The deviatoric stress can be presented by assuming linear elastic theory and considering Hook's law as [8]

$$\frac{DS^{ij}}{Dt} = 2G\left( \dot{\varepsilon}^{ij} - \frac{1}{3}\delta^{ij}\dot{\varepsilon}^{ij} \right) + S^{ik}\omega^{jk} + \omega^{ik}S^{kj}, \tag{5}$$

where $G$ is the shear modulus. The strain rate tensor $\dot{\varepsilon}^{ij}$, and rotation tensor $\omega^{ij}$ are defined as

$$\dot{\varepsilon}^{ij} = \frac{1}{2}\left( \frac{\partial u^i}{\partial x^j} + \frac{\partial u^j}{\partial x^i} \right), \tag{6}$$

$$\omega^{ij} = \frac{1}{2}\left( \frac{\partial u^i}{\partial x^j} - \frac{\partial u^j}{\partial x^i} \right). \tag{7}$$

Substituting (4) into (3) yields

$$\frac{Du^i}{Dt} = \frac{1}{\rho} \frac{\partial S^{ij}}{\partial x^j} - \frac{1}{\rho} \frac{\partial P}{\partial x^j}. \tag{8}$$

## III. METHODOLOGY

The foundation of SPH is based on interpolation theory which indicates that any field variable $\mathbf{A}$ can be defined over a domain of interest in terms of its values at a set of discrete disordered points (so-called SPH particles) by suitable definition of an interpolation kernel. These particles carry the material properties such as density, velocity, pressure, stress etc. The exact integral representation of $\mathbf{A}$ is

$$A(\mathbf{r}) = \int_{\Omega} A(\mathbf{r}')\ \delta(\mathbf{r} - \mathbf{r}')\ d\mathbf{r}', \tag{9}$$

where $\delta(\mathbf{r} - \mathbf{r}')$ is the Dirac delta function and $\Omega$ is the computational domain. Equation (9) can be represented by integral interpolation of the quantity $\mathbf{A}$ as

$$A(\mathbf{r}) \approx \int_{\Omega} A(\mathbf{r}')\ W(\mathbf{r} - \mathbf{r}', h)\ d\mathbf{r}', \tag{10}$$

where $h$ is smoothing length proper to kernel function $W$ which represents the effective width of the kernel. The kernel has the following properties [9]

$$\begin{cases} \int_V W(\mathbf{r} - \mathbf{r}', h)\ d\mathbf{r}' = 1 \\ \lim_{h \to 0} W(\mathbf{r} - \mathbf{r}', h) = \delta(\mathbf{r} - \mathbf{r}') \end{cases}. \tag{11}$$

There are many possible choices for the kernel function. A quintic kernel normalized for two-dimensions is used in the following simulation [7]

$$W(r,h) = \frac{7}{478\pi h^2} \begin{cases} (3-s)^5 - 6(2-s)^5 + 15(1-s)^5, & 0 \le s < 1; \\ (3-s)^5 - 6(2-s)^5, & 1 \le s < 2; \\ (3-s)^5, & 2 \le s < 3; \\ 0, & s \ge 3, \end{cases} \tag{12}$$

where $s = \dfrac{|\mathbf{r}|}{h}$.

If $A(\mathbf{r}')$ is known only at a discrete set of $N$ point $\mathbf{r}_1, \mathbf{r}_2, ..., \mathbf{r}_N$ then the interpolation of quantity $\mathbf{A}$ can be approximated by a summation interpolant as follows [9]

$$A_h(\mathbf{r}) \approx \sum_{b=1}^N \frac{m_b}{\rho_b} A_b W(\mathbf{r} - \mathbf{r}', h), \tag{13}$$

where the summation index $b$ denotes a particle label and particle $b$ carries a mass $m_b$ at the position $\mathbf{r}_b$. The value of $\mathbf{A}$ at $b - \text{th}$ particle is shown by $\mathbf{A}_b$.

Derivative of $\mathbf{A}$ with respect to $x$ is given by [10]

$$\left( \frac{\partial \mathbf{A}}{\partial x} \right)_a = \frac{1}{\Phi_a} \sum_b m_b \frac{\Phi_b}{\rho_b} (\mathbf{A}_b - \mathbf{A}_a) \frac{\partial W_{ab}}{\partial x}, \tag{14}$$

where $\Phi$ is any differentiable function.

## IV. SOLUTION ALGORITHM

Solution algorithm consists of a prediction-correction scheme which is similar to three-step algorithm of Hosseini *et al.* [4]. However, the algorithm is reduced to two following consecutive steps.

### A. First step (Prediction)

Solid: In this step for solids, divergence of deviatoric stress tensor $T_s^i$, is calculated according to constitutive equation

(5).

$$T_s^i = \left(\frac{1}{\rho}\frac{\partial S^{ij}}{\partial x^j}\right)_a = \sum_b m_b \left(\frac{S_a^{ij}}{\rho_a^2} + \frac{S_b^{ij}}{\rho_b^2}\right)\cdot\nabla_a W(\mathbf{r}_{ab},h) \quad (15)$$

where $\mathbf{r}_{ab} = \mathbf{r}_a - \mathbf{r}_b$ and

$$\nabla_a W(\mathbf{r}_{ab},h) = \frac{dW}{d\mathbf{r}_{ab}}\frac{1}{|\mathbf{r}_{ab}|}\left(x_a^i - x_b^j\right). \quad (16)$$

Fluid: In this step for fluids, divergence of shear stress tensor should be calculated. Hosseini *et al.* [4,6] calculated the shear stress tensor using the second principal invariant of the shear strain rate tensor:

$$D^{ij} = \frac{1}{2}\left(\nabla u^j + \nabla u^{jT}\right), \quad (17)$$

$$\tau^{ij} = 2\mu\, D^{ij}, \quad (18)$$

$$T_f^i = \left(\frac{1}{\rho}\frac{\partial \tau^{ij}}{\partial x^j}\right)_a = \sum_b m_b \left(\frac{\tau_a^{ij}}{\rho_a^2} + \frac{\tau_b^{ij}}{\rho_b^2}\right)\cdot\nabla_a W_{ab}. \quad (19)$$

Nevertheless, results presented for the Poiseuille flow problem in the section six, indicate that the velocity profile computed using the above form of divergence of shear stress tensor is inaccurate near the boundaries. To address this problem, in this work another form of the viscous term proposed by Morris *et al.* [7] is substituted:

$$T_f^i = \left(\frac{1}{\rho}\frac{\partial \tau^{ij}}{\partial x^j}\right)_a = \sum_b m_b \left(\frac{(\mu_a + \mu_b)\,u_{ab}^i}{\rho_a\rho_b\left(\mathbf{r}_{ab}^2 + \eta^2\right)}\right)x_{ab}^i\cdot\nabla_a W_{ab}\,(20)$$

where $\eta$ is a small number to avoid singularities. Although equation (20) does not satisfy angular momentum [11], no-slip boundary condition can be imposed accurately.

Finally, the vector $T^i$ which is equal to $T_f^i$ for fluid particles, and $T_s^i$ for solid particles is used to calculate a provisional velocity filed. This new velocity filed is employed to move fluid or structure particles to a new temporary position.

$$\widetilde{u}^i = u_{t-\Delta t}^i + T^i\,\Delta t, \quad (21)$$

$$\widetilde{x}^i = x_{t-\Delta t}^i + \widetilde{u}^i\,\Delta t. \quad (22)$$

*B. Second step (Correction)*

There was no constraint to impose incompressibility in the previous step; thus, movement of particles changes the local density. New densities can be calculated using the continuity equation. Choosing $\Phi = 1$, $\mathbf{A} = u^i$, and using the provisional velocity field of the previous step, (14) gives [10]

$$\left(\frac{d\widetilde{\rho}}{dt}\right)_a = \rho_a \sum_b \frac{m_b}{\rho_b}\left(\widetilde{u}_a^i - u_b^i\right)\cdot\nabla_a W(\mathbf{r}_a - \mathbf{r}_b, h). \quad (23)$$

This equation states that when two particles approach each other, their relative velocity and the gradient of kernel function have the same signs, consequently $D\widetilde{\rho}_a/Dt$ will be positive and $\widetilde{\rho}_a$ will increase and vice versa. Through combination of the pressure gradient term of the momentum equation and continuity equation, a Poisson equation is formulated by which a trade off between deviation of density and pressure is produced [12].

$$\frac{1}{\rho_0}\frac{\rho_0 - \widetilde{\rho}}{\Delta t} + \frac{\partial \hat{u}^j}{\partial x^j} = 0, \quad (24)$$

$$\hat{u}^i = -\left(\frac{1}{\widetilde{\rho}}\nabla P\right)\Delta t, \quad (25)$$

$$\nabla\cdot\left(\frac{1}{\widetilde{\rho}}\nabla P\right) = \frac{\rho_0 - \widetilde{\rho}}{\rho_0\,\Delta t^2}. \quad (26)$$

Pressure of each particle is calculated according to the following form of equation (26):

$$P_a = \left(\frac{\rho_0 - \widetilde{\rho}_a}{\rho_0\,\Delta t^2} + \sum_b \frac{8m_b}{(\widetilde{\rho}_a + \rho_b)^2}\frac{P_b x_{ab}^i\cdot\nabla_a W_{ab}}{|\mathbf{r}_{ab}|^2 + \eta^2}\right)$$
$$\Bigg/\left(\sum_b \frac{8m_b}{(\widetilde{\rho}_a + \rho_b)^2}\frac{x_{ab}^i\cdot\nabla_a W_{ab}}{|\mathbf{r}_{ab}|^2 + \eta^2}\right). \quad (27)$$

The SPH form of (25) provides the velocity field by which incompressibility is satisfied

$$\hat{u}_a^i = -\Delta t \sum_b m_b\left(\frac{P_a}{\widetilde{\rho}_a^2} + \frac{P_b}{\rho_b^2}\right)\nabla_a W_{ab}. \quad (28)$$

Finally, velocity of each particle at the end of time step will be obtained as

$$u_{t+\Delta t}^i = \widetilde{u}^i + \hat{u}^i, \quad (29)$$

and final positions of particles are calculated using a central difference scheme in time

$$x_t^i = x_{t-\Delta t}^i + \frac{\Delta t}{2}(u_t^i + u_{t-\Delta t}^i). \quad (30)$$

This step is common for both fluid and structure particles; hence, if fluid particles approach structure particles, their pressure will increase thereby structure particles move into a new position where the coupling is satisfied, and vice versa.

## V. BOUNDARY CONDITION

The desired problem involves interaction of fluid flow and elastic walls. These elastic walls must prevent penetration of fluid particles into solid boundaries. In addition, in such internal flow problems the no-slip condition needs to be satisfied. In order to ensure the no-slip condition, fluid velocity at boundary should be equal to the solid velocity at this point.

As mentioned, second step satisfies the desired anti penetration condition by increasing the pressure when two particles approaching each other. However, the no-slip boundary condition demands more attention, since unlike other past-proposed methods, which were consisted of fixed or moving rigid boundaries, in FSI problems deformable boundaries are of interest. A simple technique to implement no-slip boundary condition is usage of image particles [13]. Nevertheless, this method is usually limited to straight boundaries and simple geometries. In this paper, the velocity extrapolation method proposed by Morris *et al.* [7] is used. According to this method, velocity of each fluid particle is extrapolated to neighbor wall particles (as an artificial velocity) across the tangent plane (or tangent line in 2D) of

the boundary (Fig. 1). The unit vector of the tangent plane is

$$\hat{t}^i = \frac{x_{O+1}^i - x_{O-1}^i}{\left| x_{O+1}^i - x_{O-1}^i \right|}. \tag{31}$$

In order to implement the aforementioned method for FSI problems, it can be assumed that there are ghost particles which have similar positions as wall particles. The artificial extrapolated velocity of each wall particle is attributed to the relevant ghost particle. Other properties of these ghost particles are similar to those of fluid particles.

$$u_{b_{ghost}}^i = u_O^i + \left( d_a / d_b \right)\left( u_O^i - u_a^i \right), \tag{32}$$

The no-slip boundary condition satisfies when velocity of ghost particles as well as boundary particles are contributed to calculate viscous forces.
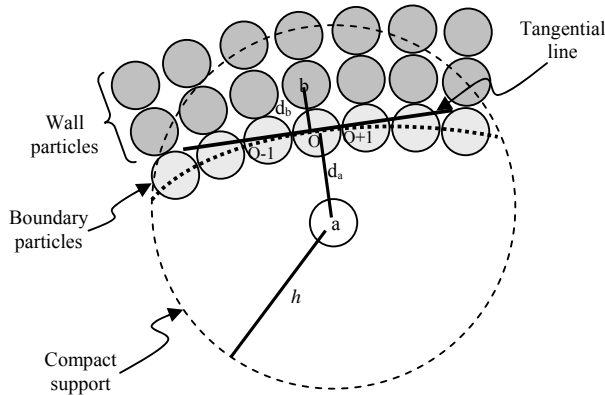


Fig. 1 Boundary condition treatment to simulate no-slip boundary condition

## VI. TEST CASES

Poiseuille flow: The Poiseuille problem consists of a fluid between two fixed plates. The fluid, which is initially at rest, is driven by a body force acting parallel to the x direction. The original configuration of the problem and its analytical solution are reported in Moriss et al. [7]. It is evident that the result of simulation based on equation (19) is highly inaccurate near the boundaries. However, when equation (20) is employed in the solution algorithm instead of equation (19), accurate velocity profile are computed.

Internal flow with FSI: The numerical test case is a two dimensional FSI simulation of a pulsatory flow moving through flexible walls. It is consisted of two flexible walls which are fixed at both ends with a length $0.09\,m$, a constant thickness $h_0 = 0.003\,m$, a radius $R_0 = 0.015\,m$, and shear module of $G = 1.5\,Mpa$. An incompressible viscous fluid, with density $\rho = 1000\,kg/m^3$ and dynamic viscosity $\mu = 0.004\,kg/m\,s$; moving inside the constructed duct with a pulsatile flow volume rate of period $T$. The time dependent velocity, which is imposed at upstream, is taken to be

$$U(t) = A + B\sin\frac{2\pi t}{T}, \tag{33}$$

where $A$ and $B$ are constant parameters selected to be 0.006 and 0.007 respectively. No-slip boundary condition is imposed on deformable walls. Square particles are selected with initial particle spacing of $\Delta x_f = 0.001\,m$, and $\Delta x_w = \Delta x_f / 2$ for fluids and solids respectively. Simulation needs several complete flow pulses to become stable. The staggered plot as well as its vector plot of velocity field is shown in Fig. 3 and Fig. 4 respectively at different stages of the pulse.
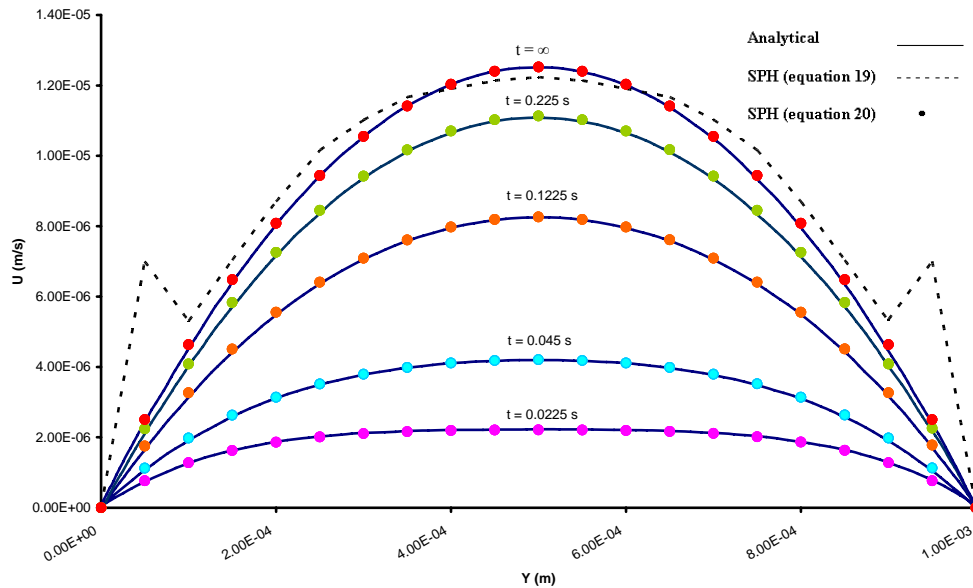


Fig. 2 Comparisons between the analytical solutions, and SPH results with two different methods for calculation of divergence of shear stress tensor
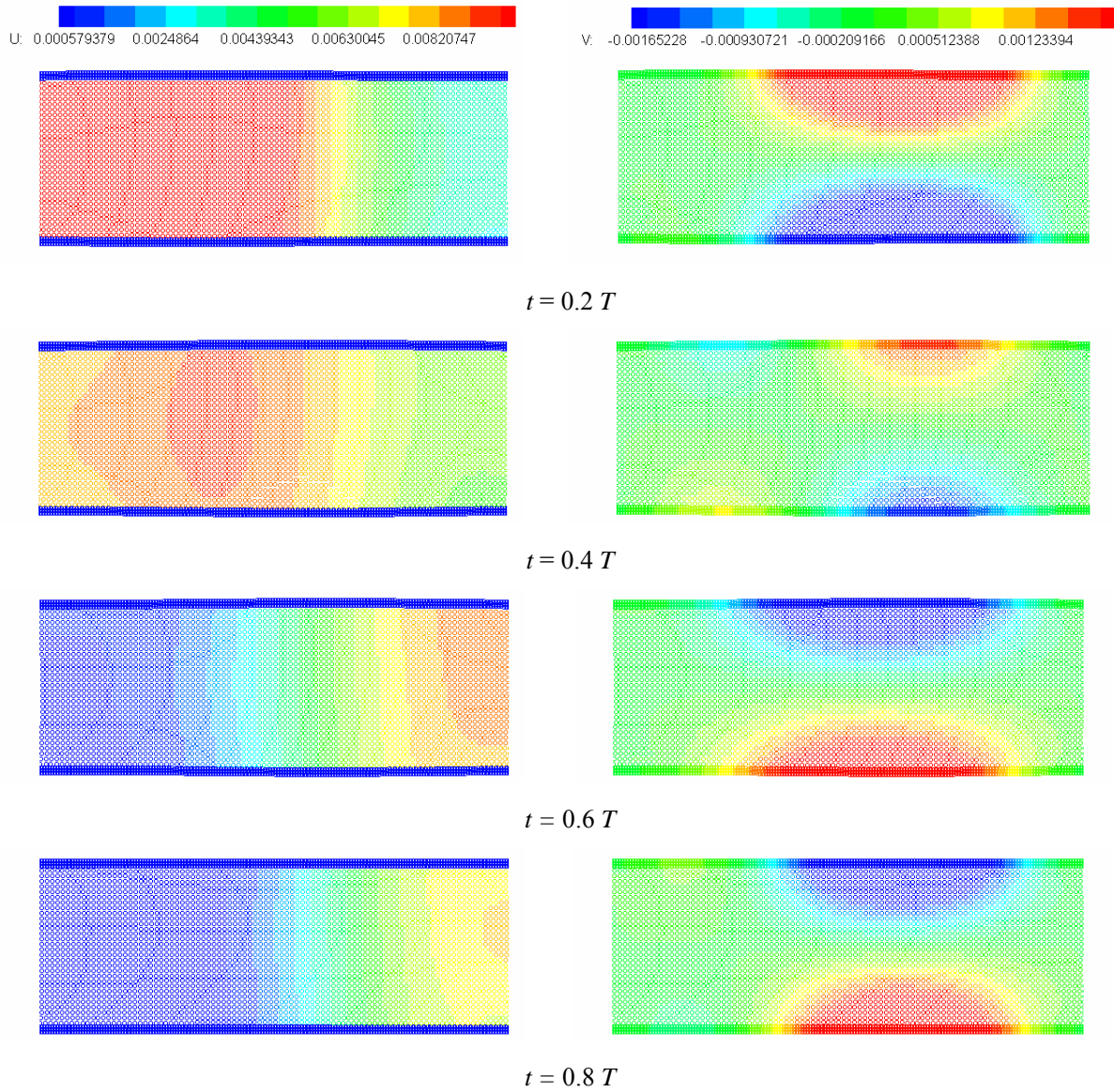
**(Advance online publication: 17 February 2009)**

U: 0.000579379    0.0024864    0.00439343    0.00630045    0.00820747

V: -0.00165228    -0.000930721    -0.000209166    0.000512388    0.00123394

*t* = 0.2 *T*

*t* = 0.4 *T*

*t* = 0.6 *T*

*t* = 0.8 *T*

Fig. 3 Staggered plot of velocity field at different stages of the flow pulse

*t* = 0.2 *T*

*t* = 0.4 *T*

*t* = 0.6 *T*

*t* = 0.8 *T*

Fig. 4 Vector plot of velocity field at different stages of the flow pulse

**(Advance online publication: 17 February 2009)**
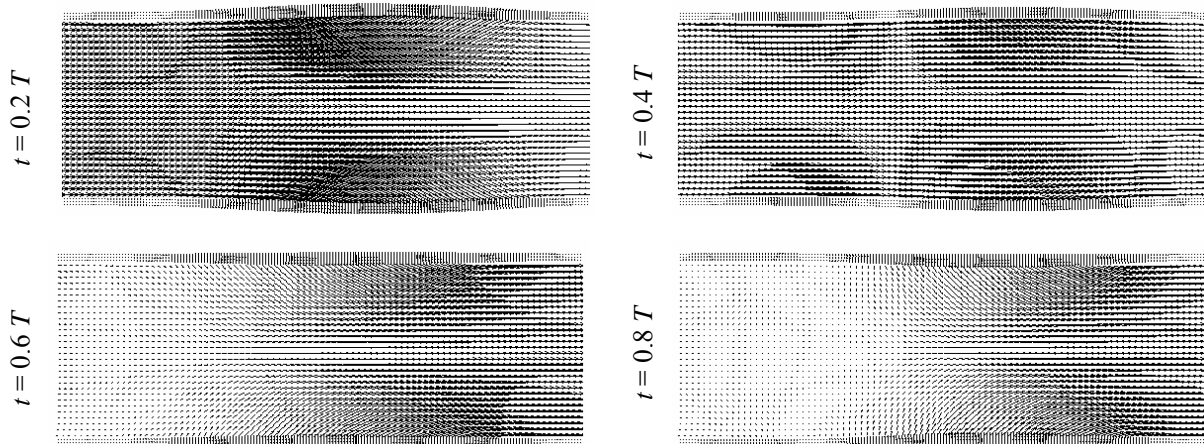
## VII. CONCLUSION

In this paper, a monolithic method for FSI problems involving no-slip boundary condition and internal fluid flows is developed using SPH. In order to improve the overall efficiency of the method, divergence of shear stress tensor for fluids is substituted with the expression proposed by Morris *et al.* [7]. Moreover, the problem of imposing no-slip boundary condition on moving boundaries is investigated using ghost particles which carry the extrapolated velocity.

## VIII. REFERENCE

[1] K. Liu, H. Radhakrishnan, V. H. Barocas, "Simulation of flow around a thin, flexible obstruction by means of a deforming grid overlapping a fixed grid," *Int. J. Numer. Meth. Fluids*, vol. 56, pp. 723-738, 2008.

[2] R. van Loon, P. D. Anderson, J. de Hart, F. P. T. Baaijens, "A combined fictitious domain/adaptive meshing method for fluid–structure interaction in heart valves," *Int. J. Numer. Meth. Fluids,* vol. 46, pp. 533–544, 2004.

[3] C. Antoci, M. Gallati, S. Sibilla, "Numerical simulation of fluid–structure interaction by SPH," *Computers and Structures*, vol. 85, pp. 879–890, 2007.

[4] S. M. Hosseini, N. Amanifard, "Presenting a modified SPH algorithm for numerical studies of fluid-structure interaction problems," *IJE Trans B: Applications*, vol. 20, pp. 167-178, 2007.

[5] M. H. Farahani, N. Amanifard, H. Asadi, M. Mahnama, "Fluid-Structure Interaction Simulation with Free Surface Flows by Smoothed Particle Hydrodynamics" *2008 ASME International Mechanical Engineering Congress & Exposition*, October, 2008, Boston, Massachusetts, USA.

[6] S. M. Hosseini, M. T. Manzari, S. K. Hannani, "A fully explicit three step SPH algorithm for simulation of non-Newtonian fluid flow, " *Int. J. of Numerical Methods for Heat and Fluid Flow*, vol. 17, pp. 715–735, 2007.

[7] J. P. Morris, P. J. Fox, Y. Zhu, "Modeling low Reynolds number incompressible flows using SPH," *J. Comp. Phys.* Vol. 136, pp. 214–226, 1997.

[8] J. Gray, J. J. Monaghan, R. P. Swift, "SPH elastic dynamics," *Comput. Methods Appl. Mech. Eng.* Vol. 190, pp. 6641–6662, 2001.

[9] J. J. Monaghan, "Smoothed particle hydrodynamics," *Ann. Rev. Astron. Astrophys.* vol. 30, pp. 543–574, 1992.

[10] J. J. Monaghan, "Smoothed particle hydrodynamics," *Rep. Prog. Phys.*, vol. 68, pp. 1703–1759, 2005.

[11] D. Violeau, R. Issa, "Numerical modelling of complex turbulent free-surface flows with the SPH method: an overview," *Int. J. Numer. Meth. Fluids*, vol. 53, pp. 277–304, 2007.

[12] E. Y. M. Lo, S. Shao, "Simulation of near-shore solitary wave mechanics by an incompressible SPH method," *Applied Ocean Research*, vol. 24, pp. 275–286, 2002.

[13] L. D. Libersky, A. G. Petschek, T. C. Carney, J. R. Hipp, F. A. Allahdadi, "High strain Lagrangian hydrodynamics," *J. Comput. Phys.* vol. 109, pp. 67-75, 1993.